

AD 742275

280



contributing to man's  
understanding of the environmental world

D D C  
RECEIVED  
26 MAY 1972  
D.

# ***SOME APPLICATIONS OF A MIXED SIGNAL PROCESSOR***

**R. H. SHUMWAY**  
**CONSULTANT TO THE SEISMIC DATA LABORATORY**

**5 JANUARY 1972**

**Prepared for**  
**AIR FORCE TECHNICAL APPLICATIONS CENTER**  
**Washington, D.C.**

**For**  
**Project VELA UNIFORM**

**Sponsored by**  
**ADVANCED RESEARCH PROJECTS AGENCY**  
**Nuclear Monitoring Research Office**  
**ARPA Order No. 1714**

**TELEDYNE GEOTECH**

Reproduced by  
**NATIONAL TECHNICAL  
INFORMATION SERVICE**  
Springfield, Va. 22151

**ALEXANDRIA LABORATORIES**

**APPROVED FOR PUBLIC RELEASE; DISTRIBUTION UNLIMITED.**

50

ADDITIONAL TO	
FORM	WHITE SECTION <input checked="" type="checkbox"/>
DO	BUFF SECTION <input type="checkbox"/>
UNAN.	OD. <input type="checkbox"/>
JUSTIFICATION.....	
BY.....	
DISTRIBUTION/AVAILABILITY.....	
BASE	ANAL. DIV. OF SPECIAL
A	

*Neither the Advanced Research Projects Agency nor the Air Force Technical Applications Center will be responsible for information contained herein which has been supplied by other organizations or contractors, and this document is subject to later revision as may be necessary. The views and conclusions presented are those of the authors and should not be interpreted as necessarily representing the official policies, either expressed or implied, of the Advanced Research Projects Agency, the Air Force Technical Applications Center, or the U S Government.*

Unclassified  
Security Classification

DOCUMENT CONTROL DATA - R&D		
(Security classification of title, body of abstract and indexing annotation must be entered when the overall report is classified)		
1 ORIGINATING ACTIVITY (Corporate author) TELEDYNE GEOTECH ALEXANDRIA, VIRGINIA		2a REPORT SECURITY CLASSIFICATION Unclassified 2b GROUP
3 REPORT TITLE SOME APPLICATIONS OF A MIXED SIGNAL PROCESSOR		
4 DESCRIPTIVE NOTES (Type of report and inclusive dates) Scientific		
5 AUTHOR(S) (Last name, first name, initial) Shumway, R.H. Consultant to the Seismic Data Laboratory		
6 REPORT DATE 5 January 1972	7a. TOTAL NO. OF PAGES 48	7b. NO. OF REFS 16
8a. CONTRACT OR GRANT NO. F33657-72-C-0009 b. PROJECT NO. VELA T/2706 c ARPA Order No. 1714 d ARPA Program Code No. 2F-10	9a. ORIGINATOR'S REPORT NUMBER(S) 280 9b. OTHER REPORT NO(S) (Any other numbers that may be assigned this report)	
10 AVAILABILITY/LIMITATION NOTICES <b>APPROVED FOR PUBLIC RELEASE; DISTRIBUTION UNLIMITED.</b>		
11 SUPPLEMENTARY NOTES	12 SPONSORING MILITARY ACTIVITY Advanced Research Projects Agency Nuclear Monitoring Research Office Washington, D. C.	
13 ABSTRACT A technique to process array data has been developed to determine when a second signal is hidden in the coda of a primary signal; and to estimate the waveform of the two signals. The effectiveness of the mixed-signal processor has been demonstrated by operating on various possible mixed signals formed from recordings of earthquakes at Tonga in the South Pacific and at the Fox Islands in the Aleutians. For small arrays the processor is found to be substantially superior to simple beamforming. The distortion introduced by the use of finite time filters is found to be negligible.		
14 KEY WORDS Signal Estimation Maximum Likelihood		

Unclassified  
Security Classification

SOME APPLICATIONS OF A MIXED SIGNAL PROCESSOR

SEISMIC DATA LABORATORY REPORT NO. 280

AFTAC Project No.:	VELA T/2706
Project Title:	Seismic Data Laboratory
ARPA Order No.:	1714
ARPA Program Code No.:	2F-10
Name of Contractor:	TELEDYNE GEOTECH
Contract No.:	F33657-72-C-0009
Date of Contract:	01 July 1971
Amount of Contract:	\$ 1,314,000
Contract Expiration Date:	30 June 1972
Project Manager:	Royal A. Hartenberger (703) 836-7647

P. O. Box 334, Alexandria, Virginia

**APPROVED FOR PUBLIC RELEASE; DISTRIBUTION UNLIMITED.**

## ABSTRACT

A technique to process array data has been developed to determine when a second signal is hidden in the coda of a primary signal and to estimate the waveforms of the two signals. The effectiveness of the mixed signal processor has been demonstrated by operating on various possible mixed signals formed from recordings of earthquakes at Tonga in the South Pacific and at the Fox Islands in the Aleutians. For small arrays the processor is found to be substantially superior to simple beam-forming. The distortion introduced by the use of finite time filters is found to be negligible.

## TABLE OF CONTENTS

	Page No.
ABSTRACT	
INTRODUCTION	1
GENERAL THEORY	6
WINDOW THEORY FOR TWO-SIGNAL FILTERS	9
ESTIMATION AND DETECTION CAPABILITIES AT TFO	13
SUMMARY	18
REFERENCES	19

## LIST OF FIGURES

Figure Title	Figure No.
Array configuration for TFO	1
Comparison of distortion introduced by truncated optimum filters and ordinary beamforming. 19 Channels at TFO with Tonga as $S_1(.)$ and Fox as $S_2(.)$ .	2
Comparison of distortion introduced by truncated optimum filters and ordinary beamforming. Seven channels (21-27) with $S_1(.)$ at 17 km/sec, 308 degrees and $S_2(.)$ at 23 km/sec, 300 degrees.	3
Comparison of distortion introduced by truncated optimum filters and ordinary beamforming. Seven channels (21-27) with $S_1(.)$ at 17 km/sec, 308 degrees and $S_2(.)$ at 23 km/sec, 240 degrees.	4
Comparison of distortion introduced by truncated optimum filters and ordinary beamforming. Three channels at TFO with $S_1(.)$ 20 km/sec, 0 degrees and $S_2(.)$ at 10 km/sec, 20 degrees.	5
Comparison of distortion introduced by truncated optimum filters and ordinary beamforming. Four channels at TFO with $S_1(.)$ at 20 km/sec, 0 degrees and $S_2(.)$ at 10 km/sec, 30 degrees.	6
Analysis of Tonga $S_1(t)$ event using $N = 19$ channels recorded at TFO at high signal to noise ratio.	7
Analysis of Tonga $S_1(t)$ - Fox $S_2(t)$ mixture using $N = 19$ channels recorded at TFO at a high signal to noise ratio.	8
Analysis of Tonga $S_1(t)$ and Fox $S_2(t)$ noisy mixture using $N = 19$ channels recorded at TFO.	9
Analysis of Tonga $S_1(t)$ and Fox $S_2(t)$ mixture for $N = 19$ channels showing bias in beam formed estimate for Fox.	10a
Results of a least-squares technique for estimation of one signal in the presence of another.	10b

# LIST OF FIGURES (Cont'd.)

Figure Title	Figure No.
Frequency wave number analysis. $N = 7$ channels measuring Tonga and Fox at TFO (1.25 Hz).	11
Frequency wave number analysis. $N = 7$ noisy channels measuring Tonga and Fox at TFO (1.25 Hz).	12
Maximum likelihood estimate for Tonga using Tonga-Fox mixture in $N = 7$ channels at TFO (Figure 8) with various possible azimuths for Tonga.	13
F statistics for detecting Tonga in Tonga-Fox mixture ( $N = 7$ center elements at TFO).	14
Maximum likelihood estimate for Tonga using Tonga-Fox mixture in $N = 7$ noisy channels at TFO with various possible azimuths for Tonga.	15
F statistic for detecting Tonga in Tonga-Fox noisy mixture ( $N = 7$ center elements at TFO).	16



## LIST OF TABLES

Table Title	Table No.
Values of F Testing for the Presence of Fox in Data Containing Only Tonga	I
Values of F Testing for the Presence of the Fox Island Signal in Data Containing Both Fox Island and Tonga Signals.	II
Values of F Testing for the Presence of the Fox Island Signal in Noisy Data Containing Both Fox Island and Tonga Signals.	III
Values of F Testing for the Presence of the Tonga Signal in Data Containing Both Tonga and Fox Island Signals.	IV

## INTRODUCTION

A number of complications are introduced into signal estimation and detection procedures when one is willing to admit the possibility of interfering waveforms. This may occur when a propagating noise, generated perhaps by a storm, appears on a seismic record simultaneously with a propagating signal from an earthquake or explosion. It may occur when signals from an explosion (accidentally or purposefully) coincide with those from an earthquake of an appropriate magnitude, depth and location. Either of the above phenomenon causes one to re-evaluate the applicability of the single signal plus noise model

$$H_1: Y_j(t) = S_1(t - T_{j1}) + n_j(t) \quad (1)$$

for  $j = 1, \dots, N$  time series sampled at  $T$  points  $t = 0, 1, \dots, T-1$ , where the plane wave signal suffers a time delay  $T_{j1}$  at the  $j^{\text{th}}$  sensor. In (1) when the noise processes are independent (i.e.  $n_j(t)$  and  $n_k(t)$  are independent for  $j \neq k$ ) with equal autocorrelation functions, it is well-known (Kelly, 1965), (Shumway and Dean, 1968) that a simple beam produces the minimum variance linear undistorted estimate of the signal. Furthermore, an approximation to the likelihood detector can be derived under either of two assumptions, namely

(a) The noise series are stationary Gaussian and their noise autocorrelation (spectrum) is known exactly.

(b) The noise series are stationary Gaussian and their noise autocorrelation (spectrum) is unknown.

In case (a) the detection statistic is proportional to the ratio of the beam power to the known noise power and has asymptotically a chi-square distribution with  $2BT$  degrees of freedom where  $B$  is the bandwidth and  $T$  is the sampling interval. If the data are assumed to be stationary over a long period before the signal arrives, the known noise spectrum may be replaced with an estimated one and the resulting test statistic will converge in distribution to a chi-square variable with  $2BT$  degrees of freedom as before. This procedure is basic to the on-line detector in operation at LASA (Kobayashi and Welch, 1970). It should be noted that the consequences of a change in the noise spectrum within the signal window, e.g. a seismometer noise burst, may be serious if this detector is employed.

If assumption (b) is made, one treats the spectrum of the noise series as an unknown parameter in the likelihood equations so that an estimate of the noise spectrum is made within the signal window. One finds this procedure, in the time domain, described in early works of Melton, et al. (1957) and Booker (1965). The time domain representation necessitated the assumption that  $n_j(t)$  was a white noise process. Failure of this method initially can now be ascribed to a combination of instrumentation, small arrays resulting in correlated noise, and non-white noise over the band of interest. The method is re-formulated in the frequency domain by Shumway (1970), (1971) and Shumway

and Husted (1970) where it is shown that the ratio of the beam power to the estimated noise spectrum converges in distribution to a non-central F distribution with  $2BT$  and  $2BT(N-1)$  degrees of freedom and a non-centrality parameter proportional to the signal to noise ratio and number of time series,  $N$ . This enables one to approximate the signal detection probabilities for a fixed false alarm rate as a function of signal to noise ratio. The F detector, coined by Melton, the Fisher detector, has been applied by Blandford (1970) at TFO; he provides computational procedures for setting the theoretical detection performance characteristics and shows that results can be achieved which compare favorably with those of skilled analysts reading film data. Cases where off beam events fail to give false alarms with the Fisher detector are shown.

An extension of the model implied by assumption (a) was given by Capon et al. (1967) who assumed that the noise was correlated between sensors implying a known spectral matrix. The approximate likelihood estimate for the signal in this case is weighted by convolution with a vector impulse response function proportional to the inverse of the known spectral matrix. The potential effectiveness of this method is blunted somewhat by the lack of a correlation in a well spaced array and the difficulty of forming an estimate of the spectral matrix which does not change over time for a closely spaced array.

An example of a multiple signal model is the two

signal model

$$H_2: Y_j(t) = S_1(t-T_{j1}) + S_2(t-T_{j2}) + n_j(t) \quad (2)$$

with  $S_2(t)$  a second propagating plane wave. Development of multiple signal models proceeded somewhat more slowly due in part to the lack of a fast Fourier transform algorithm and in part to a failure to realize that most multiple signal models can be treated as variants of the time series regression model of Bendat and Piersol,(1966). In the multivariate generalization (Shumway and Dean, 1968) of this model, we regard  $(Y_j(t), j = 1, \dots, N)$  as a collection of output series related to a collection of input series (deterministic functions) through a collection of impulse response functions (signals)  $(S_j(t), j = 1, \dots, P)$  which are to be estimated. The appropriate model is for  $(t = 0, \pm 1, \pm 2, \dots)$

$$Y_j(t) = \sum_{u=-\infty}^{\infty} \sum_{k=1}^P x_{jk}(t-u) S_k(u) + n_j(t) \quad (3)$$

where the choice  $P = 2, x_{jk}(t) = \delta(t-T_{jk})$

$$j = 1, \dots, N, K = 1, 2 (\delta(t) = 1$$

for  $t = 0$  and zero otherwise) reduces (3) to equation (2). An early application of this technique by Dean (1966) was later described in Shumway and Dean (1968). Similar solutions to the estimation problem posed by the special case of (3), which yields the two-signal model (2), can be found in Schweppe (1968) and Kobayashi

and Welch (1970). The asymptotic detection theory for the case of  $P$  signals present, according to the signal and noise model (3), is given in Shumway (1970) where it is shown that the ratio of signal power to noise power appropriate for testing hypothesis  $H_1$  given by (1) against  $H_2$  given by (2), converges in distribution to a non-central  $F$  distribution with  $2BT P$  and  $2BT(N-P)$  degrees of freedom.

In this report, we will analyze in more detail the detection and estimation capabilities of the two-signal model. This will include a case where two signals arriving at TFO are mixed at high and low signal to noise ratios. A large array consisting of 19 elements and two small arrays containing seven and three elements respectively are considered for signals from Fox Island in the Aleutians and from Tonga Island in the South Pacific. We investigate the distortion introduced using the finite time truncated filters by calculating and displaying the "window" through which the true signals are viewed. Various velocities, azimuths and subarray choices are evaluated both with respect to the distortion introduced and with respect to the detection performance. An analysis of the two events is made with the second signal assumed to be present at various fixed azimuths and velocities. This indicates that the two-signal model could be used as a possible substitute for a frequency wave number plot if a primary signal or noise source of fixed azimuth and velocity could be identified as the first signal.

## GENERAL THEORY

To test the hypothesis that the second signal is absent in the model given by equation (2) i.e. (2) against (1), we need the likelihood estimates for  $S_1(t)$  and  $S_2(t)$  under  $H_1$  and  $H_2$ . Consider first the solution under  $H_2$ , say

$$S_j^{++}(t) = \sum_{k=1}^N \sum_{u=0}^{T-1} h_{jk}(t-u) Y_k(u) \quad (4)$$

where  $j = 1, 2$ . Suppose that the zero mean noise process  $n_j(t)$  is weakly stationary and Gaussian with a continuous bounded spectrum determined by

$$E[n_j(t)n_j(t')] = \int_{-\pi}^{\pi} P_{nn}(\omega) e^{i\omega(t-t')} \frac{d\omega}{2\pi} \quad (5)$$

where  $P_{nn}(\cdot)$  denotes the power spectrum of the noise assumed to be the same for each  $j = 1, \dots, N$ . Furthermore,  $n_k(t)$  is assumed to be uncorrelated with  $n_j(t)$ . Now, using the fact that the two signal model (5) is a special case of (3), the transformed version of the filter in (4) is given (Shumway and Dean, 1968) by

$$\begin{aligned} H_{1k}(\omega) &= \Delta^{-1}(\omega) (N e^{i\omega T_{k1}} - \Lambda(\omega) e^{i\omega T_{k2}}) \\ H_{2k}(\omega) &= \Delta^{-1}(\omega) (N e^{i\omega T_{k2}} - \Lambda^*(\omega) e^{i\omega T_{k1}}) \end{aligned} \quad (6)$$

with

$$\Delta(\omega) = N^2 - |A(\omega)|^2 \quad (7)$$

and

$$A(\omega) = \sum_{j=1}^N e^{i\omega(T_{j1} - T_{j2})} \quad (8)$$

We take  $\Pi_{1k}(0) = \Pi_{2k}(0) = (2N)^{-1}$  to eliminate the singularity introduced by  $\Delta(0) = 0$ . Under hypothesis  $\Pi_1$  the estimates are  $S_2^+(t) = 0$  and

$$S_1^+(t) = N^{-1} \sum_{j=1}^N Y_j(t + T_{j1}) \quad (9)$$

The form of the likelihood detector for testing  $\Pi_1$  against  $\Pi_2$  depends upon (Shumway, 1970) reconstructing the noise traces at each level using the estimated signals under  $\Pi_1$  and  $\Pi_2$ . This implies that

$$n_j^+(t) = Y_j(t) - S_1^+(t - T_{j1}) \quad (10)$$

and

$$n_j^{++}(t) = Y_j(t) - S_1^{++}(t - T_{j1}) - S_2^{++}(t - T_{j2}) \quad (11)$$

If we then define the estimated spectra of the two predicted noise processes as  $P_{n_j n_j}^+(\omega)$  and  $P_{n_j n_j}^{++}(\omega)$  respectively, the average noise spectra under  $\Pi_1$  and



$H_2$  would be

$$p_{nn}^*(\omega) = N^{-1} \sum_{j=1}^N p_{n_j n_j}^*(\omega) \quad (12)$$

and

$$p_{nn}^{**}(\omega) = N^{-1} \sum_{j=1}^N p_{n_j n_j}^{**}(\omega) \quad (13)$$

Suppose, then, that a subset of  $L$  frequencies (a band of width  $B$ ) about the point  $\omega$  can be found such that  $p_{nn}^*(.)$  and  $p_{nn}^{**}(.)$  are approximately constant over that subset (band). Then, an  $F$  statistic with  $2BT$  and  $2BT(N-2)$  degrees of freedom is given approximately by

$$F(2BT, 2BT(N-2)) \approx \frac{p_{nn}^*(\omega) - p_{nn}^{**}(\omega)}{p_{nn}^{**}(\omega)} (N-2) \quad (14)$$

if  $H_1$  is true where  $p_{nn}^*(\omega)$  and  $p_{nn}^{**}(\omega)$  now represent spectral estimates smoothed over the bandwidth of interest, the numerator of (14) measures the improvement in going from the one signal to the two signal model. If the alternate hypothesis  $H_2$  is true, (14) becomes a non-central  $F$  with non-centrality parameter proportional to  $\Delta(\omega)$  and the average noise power spectrum of the second signal over the band of interest.

Before proceeding to detailed examples, involving seismic data, we examine the resolution and bias of the truncated time maximum likelihood filters.

## WINDOW THEORY FOR TWO-SIGNAL FILTERS

Since the maximum likelihood filters (5) are unbiased only for the case where infinite two-sided operators can be constructed, it is reasonable to ask how well the truncated time versions reproduce the signal of interest. This was accomplished by noting that the expected value of any filter output which estimates  $S_j(t)$  (see (4) for example) may be expressed as

$$E[S_j(t)] = \sum_{u=0}^{T-1} F_{1j}(t-u)S_1(u) + \sum_{u=0}^{T-1} F_{2j}(t-u)S_2(u) \quad (15)$$

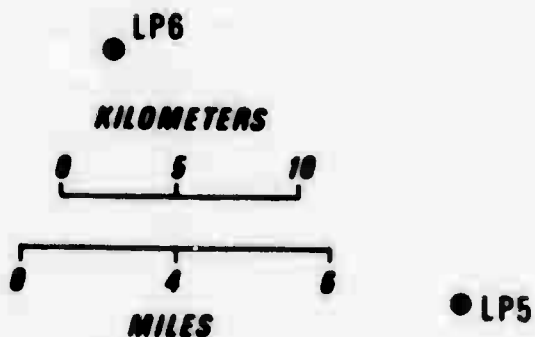
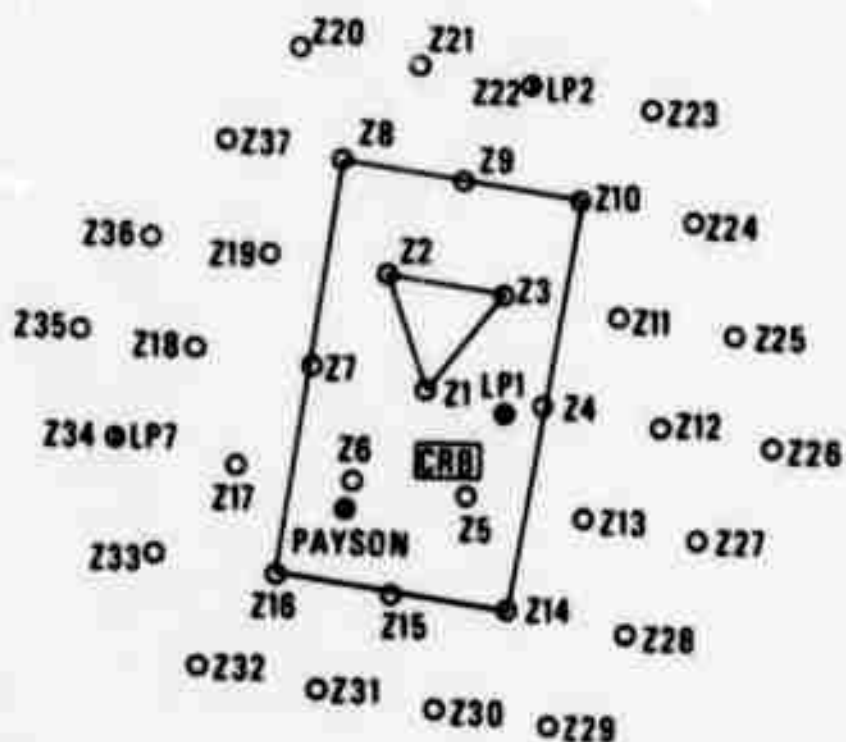
for  $j = 1, 2$ . For example, with  $j = 1$ ,  $F_{11}(t)$  is the transfer function which relates the true signal 1 to the estimated signal 1 and  $F_{21}(t)$  is the transfer function showing the amount of signal 2 which leaks into the estimate for signal 1. In the ideal case  $F_{11}(t)$  would be a unit spike at zero and  $F_{21}(t)$  would be zero for all  $t$ . The deviation from these idealized values for the "window" functions  $F_{11}(\cdot)$  and  $F_{21}(\cdot)$  measures the distortion or bias of the filters. Similarly,  $F_{12}(t)$  is the amount of signal 1 leaking into the signal 2 estimate and  $F_{22}(t)$  is the amount of signal 2 appearing in the estimate for signal 2. The  $2 \times 2$  matrix of time functions characterizes the bias of the filters in the same way that the spectral window function characterizes the bias of the various

methods for estimating the power spectrum.

In order to compare the bias of the maximum likelihood filters with the bias of ordinary beam forming over a reasonable range of initial conditions, an array of 19 elements at TFO (Figure 1), was chosen and it was assumed that signals were arriving with velocities near 20 km per second on azimuths distributed about the circle.

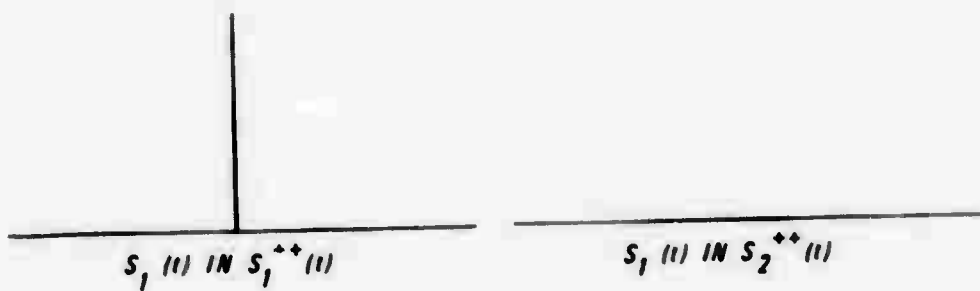
As a first test case, it was assumed, as in subsequent examples to be given later, that signals from Fox Island in the Aleutians and Tonga in the South Pacific arrive at all 19 elements and are filtered under  $H_1(+)$  (ordinary beam forming) and  $H_2(++)$  (maximum likelihood). Figure 2 shows the distortion introduced and we note that the maximum likelihood procedure produces virtually no distortion. In the beam forming, the two signals are not distorted by their own waveforms but signal 1 receives a small component from signal 2 and vice versa. One could envision severe distortion only in the case where the amplitude of signal 2 is high relative to signal 1 or vice versa. The signals are well separated in velocity and azimuth so that one would not expect problems using either procedure.

In order to examine distortion on a somewhat smaller array, the seven center elements ( $z_1 - z_7$  in Figure 1) were chosen and it was assumed that signal 1 arrived at a velocity of 17 km/sec and azimuth of 308 degrees. The second signal was assumed to have a velocity of 23 km/sec

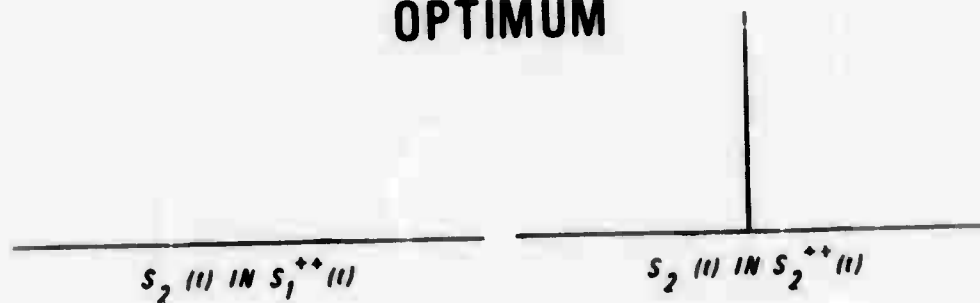


- ① THE ○ CIRCLES LABELED Z1 THROUGH Z37 ARE CENTERED ON THE 37 SHORT PERIOD SEISMOMETER LOCATIONS.
- ② THE ● CIRCLES LABELED LP1 THROUGH LP7 ARE CENTERED ON THE 7 THREE - COMPONENT LONG PERIOD SEISMOMETERS.
- ③ THE **CRB** IS THE CENTRAL RECORDING BUILDING.

Figure 1. Array configuration for TPO.



## OPTIMUM



## BEAM FORMED

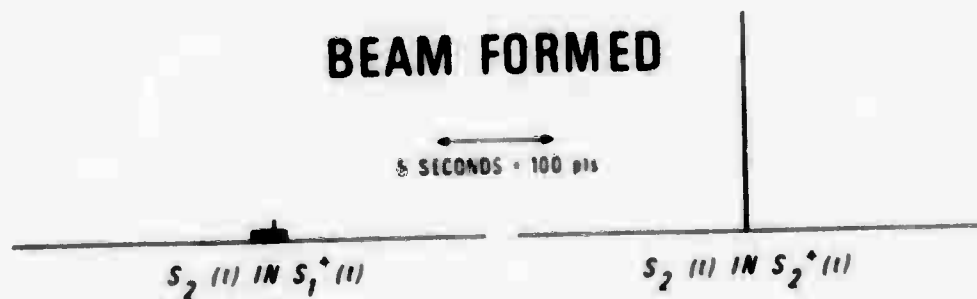


Figure 2. Comparison of distortion introduced by truncated optimum filters and ordinary beamforming. 19 channels at 110 with fonga as  $S_1(f)$  and fona as  $S_2(f)$ .

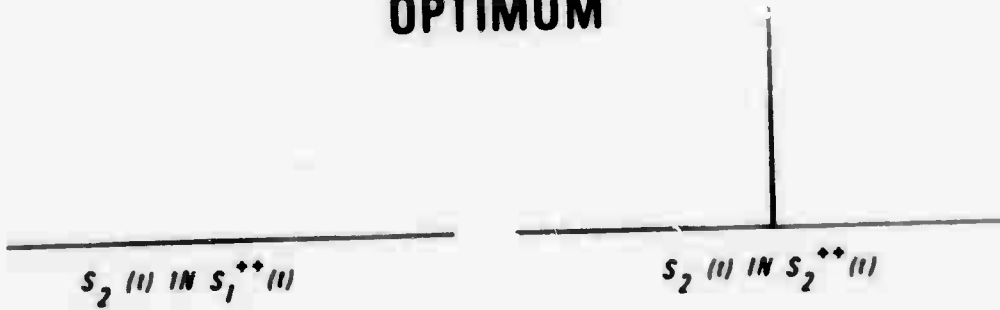
and a collection of 19 different azimuths running from 0 to 360 degrees were investigated. In general, the results were the same as for Figure 2 except that the side lobes of the beam distortion are  $1/8$  the peak. Two interesting worst cases appear. The first case in Figure 3 shows the distortion when the second signal is at 300 degree azimuth, i.e. separated 8 degrees in azimuth and 6 km/sec in velocity from signal 1. The maximum likelihood filters are relatively undistorted in this case but the beamforming filters show a definite bias. A case where the likelihood filters give more bias is shown in Figure 4 although one can see that the bias introduced is still negligible when compared with that introduced by the beam. Figure 4 corresponds to the approximate velocities and azimuths of the Tonga and Fox events.

In order to see how far it is possible to go before the distortion gets large, the three center elements z1, z2 and z3 were investigated for a number of different velocities and azimuths. Figure 5 shows a case where the two signals are separated by 10 km per second in velocity and 30 degrees in azimuth. We see that the likelihood filters still produce a relatively undistorted signal. Figure 6 shows the worst distortion ever produced by the likelihood filters. In this case, the elements z8, z10, z14 and z16 were investigated at the same velocity azimuth separation as in Figure 4. It is evident that some leakage can occur in the worst cases.

To summarize the results of the preceding discussion, we remark that for most combinations of velocities and



## OPTIMUM



## BEAM FORMED

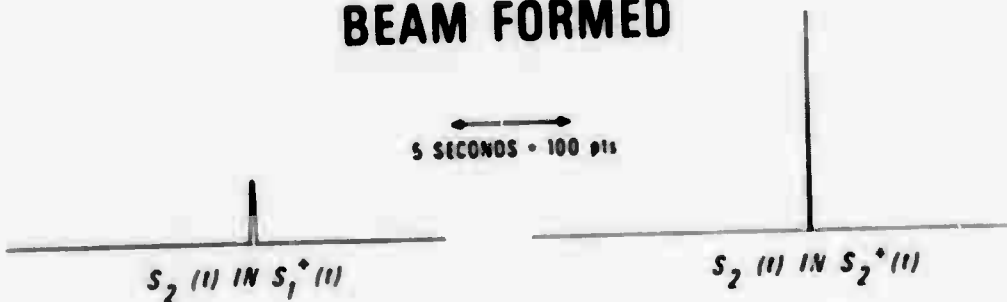
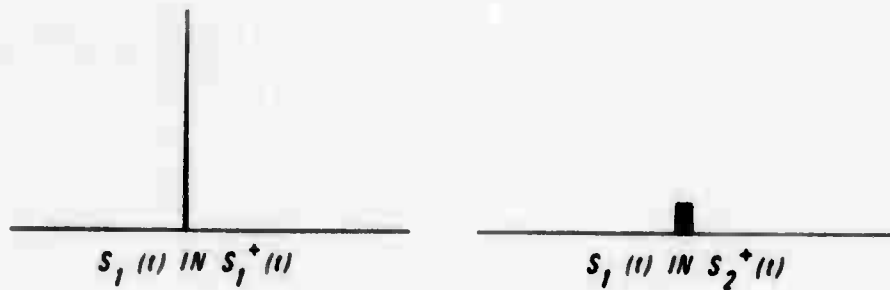
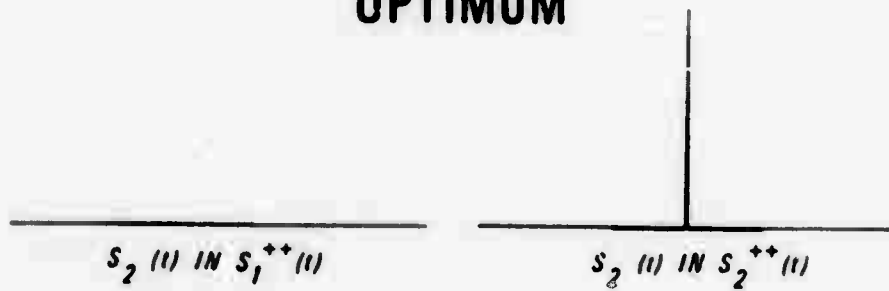


Figure 3. Comparison of distortion introduced by truncated optimum filters and ordinary beamforming. Seven channels (21-27) with  $S_1(\cdot)$  at 17 kn/sec, 300 degrees and  $S_2(\cdot)$  at 23 kn/sec, 300 degrees.



## OPTIMUM

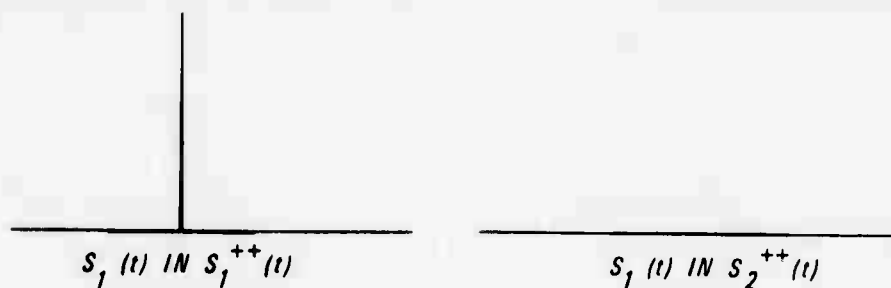


## BEAM FORMED

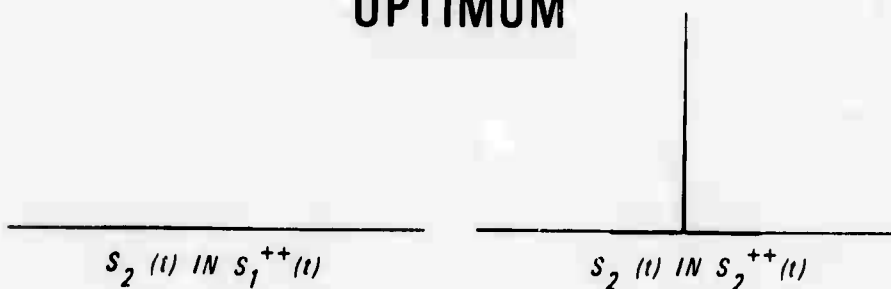


Figure 4. Comparison of distortion introduced by truncated optimum filters and ordinary beamforming. Seven channels (21-27) with  $S_1(\cdot)$  at 17 km/sec, 308 degrees and  $S_2(\cdot)$  at 23 km/sec, 240 degrees.





## OPTIMUM



## BEAM FORMED

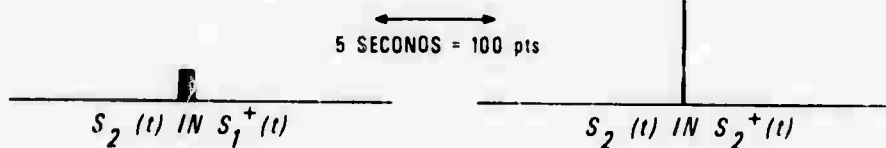
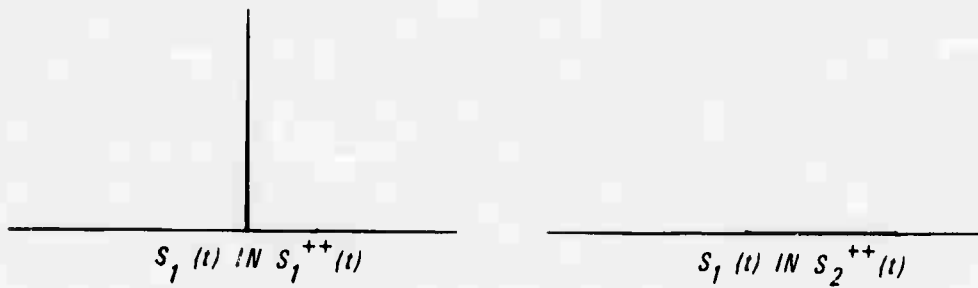
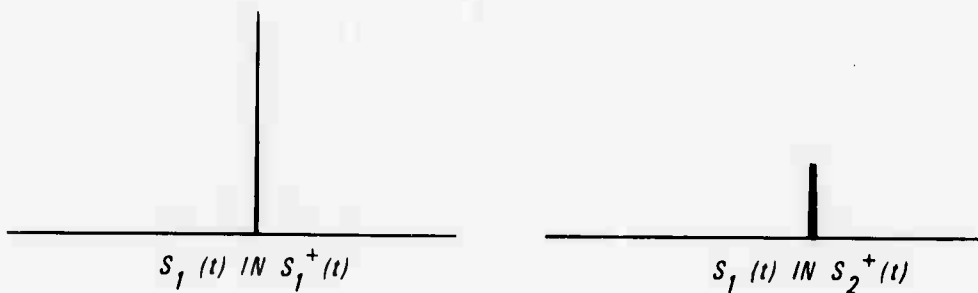
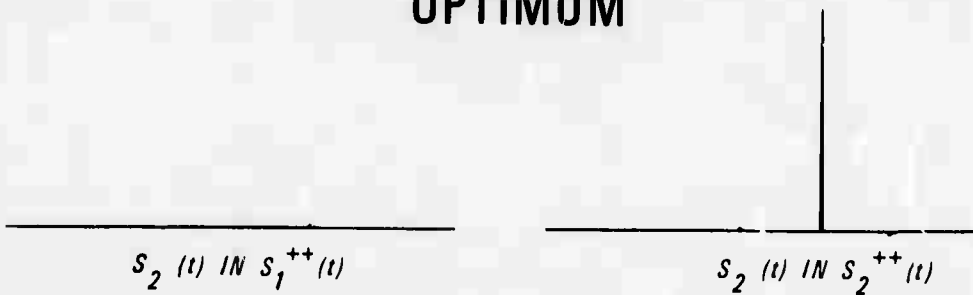


Figure 4. Comparison of distortion introduced by truncated optimum filters and ordinary beamforming. Seven channels (21-27) with  $S_1(\cdot)$  at 17 km/sec, 308 degrees and  $S_2(\cdot)$  at 23 km/sec, 240 degrees.



## OPTIMUM



## BEAM FORMED

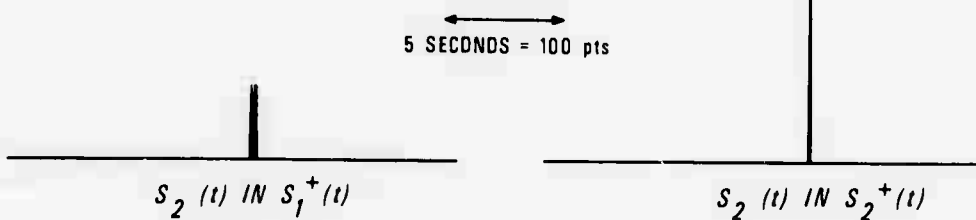
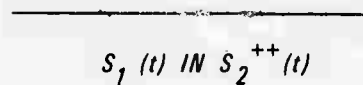
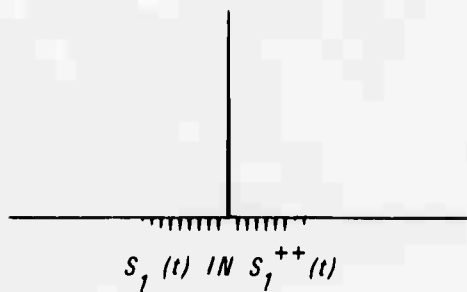
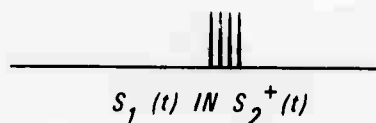
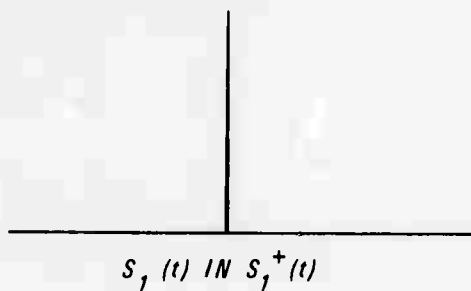
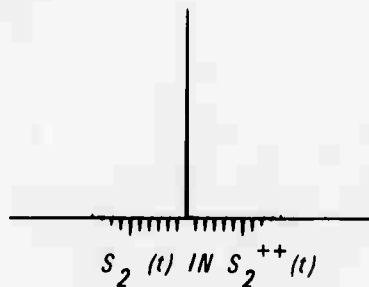


Figure 5. Comparison of distortion introduced by truncated optimum filters and ordinary beamforming. Three channels at TFO with  $S_1(\cdot)$  20 km/sec, 0 degrees and  $S_2(\cdot)$  at 10 km/sec, 20 degrees.



## OPTIMUM



## BEAM FORMED

5 SECONDS = 100 pts

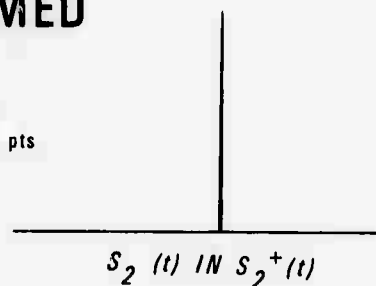
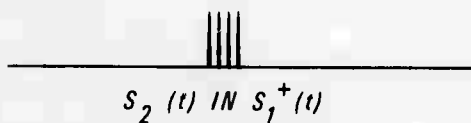


Figure 6. Comparison of distortion introduced by truncated optimum filters and ordinary beamforming. Four channels at TFO with  $S_1(\cdot)$  at 20 km/sec, 0 degrees and  $S_2(\cdot)$  at 10 km/sec, 30 degrees.

azimuths the distortion introduced by the maximum likelihood filters is remarkably small. The limit on the techniques performance in practice will probably arrive from lack of signal correlation from sensor to sensor. This might cause the contamination between signals to be greater than that shown in Figures 2-6. The window computation of this section provides a method for evaluating the signal separating capability of a subarray relative to two plane waves propagating with a given velocity and azimuth. In fact, if certain subarrays are chosen for monitoring areas which might be conducive to hiding explosions in earthquakes, the window computation can determine the proper location, configuration and spacing of the subarray needed to resolve the two signals. An extension of the technique to take account of the loss of signal correlation with distance would be needed to design the optimum array in practice.

## ESTIMATION AND DETECTION CAPABILITIES AT TFO

In this section we investigate in more detail a test set of data consisting of a mixture of an event from Fox Island and an event from Tonga. The real signals are mixed with real noise from TFO at high and low signal to noise ratios. The velocities and azimuths are approximately 17 km/sec and 308 degrees for Fox Island and 23 km/sec and 241 degrees for Tonga. It is frequently convenient to interchange the numbering of the Tonga and Fox signals, so a certain amount of caution should be exercised in reading the following discussion.

Consider first, a case where 19 channels of data are available at a very high signal to noise ratio. Figure 7 shows a case where only the Tonga Island (in this case  $S_1(.)$ ) is present at a high signal to noise ratio. The 19th channel is shown along with the maximum likelihood estimates  $S_1^{++}(.)$  and  $S_2^{++}(.)$  under  $H_2$ . Of course, the Fox Island signal (in this case  $S_2(.)$ ) is not present and  $S_2^{++}(.)$  shows that some activity is present possibly at the second signal velocity. However, when the  $y_j(t)$  is reconstructed, say, by  $y_j^{++}(t)$ , the value of the F statistic, which must be exceeded in order to reject the hypothesis that  $S_2(.)$  is absent at the .99 probability level, is 2.48. This significance value is not exceeded at any frequency as can be seen from the computed F statistics in Table I. Therefore, we accept the hypothesis that the Tonga signal is absent. Now a second data array was

$$\begin{aligned} & \delta(t+T_{1,19}) \\ & h_{1,19}(t) \\ & h_{2,19}(t) \end{aligned}$$

$$Y_{19}(t)$$

$$Y_{19}^{++}(t) = S_1^{++}(t-T_{1,19}) + S_2^{++}(t-T_{2,19})$$

$$\begin{aligned} & S_1^{++}(t) \\ & S_2^{++}(t) \end{aligned}$$

5 SECONDS = 100 pps

Figure 7. Analysis of Tonga S1(t) event using  $N = 19$  channels recorded at TFO at high signal to noise ratio. Channels are normalized to equal peak-to-peak amplitude.

TABLE 1  
Values of F Testing for the Presence of  
Fox in Data Containing Only Tonga

<u>Hz (cps)</u>	<u>F</u>
.156	1.89730
.313	.99805
.469	1.96731
.625	2.10992
.781	.89259
.938	.97330
1.094	1.02410
1.250	.98761
1.406	1.02226
1.563	.95154
1.719	.61049
1.875	.60003

made up which contained the signals from both Tonga and Fox Island, with the results given in Figure 8 and Table II. We note from Figure 8 that good reproductions of both signals are obtained as well as a good reconstructed trace  $y_{19}^{**}(t)$ . The F statistic rejects the absence of the Tonga signal at a very high level of significance. We include in Figure 8 the estimates for the Tonga and Fox events obtained by beamforming the original events before they are mixed. These can serve as reference signals against which to judge the effectiveness of future experiments using mixed noisy data. As an example, we consider the noisy data in Figure 9 where neither signal is visible on the original trace  $y_{19}(t)$ . The filtered traces enhance the signal fairly well and the F statistic is still significant as can be seen from Table III. Thus, it is reasonable to assume that a signal (Fox) inbedded in the code of another signal (Tonga) can be detected using the full array.

In order to examine a case where the effects of distortion can be seen on the straight beam, the roles of the Tonga and Fox Island signals were interchanged within the program. In Figure 10a we see that the beam formed estimate  $S_2^*(.)$  contains a definite contribution from the initial cycles of the Tonga event, while the maximum likelihood filters reject this component. This shows that the distortion predicted by Figure 2 can be a real factor for seismic signals. For the purpose of future reference, we give the values of the F statistic in Table IV. The strong component of the Tonga signal at 1.25 Hz



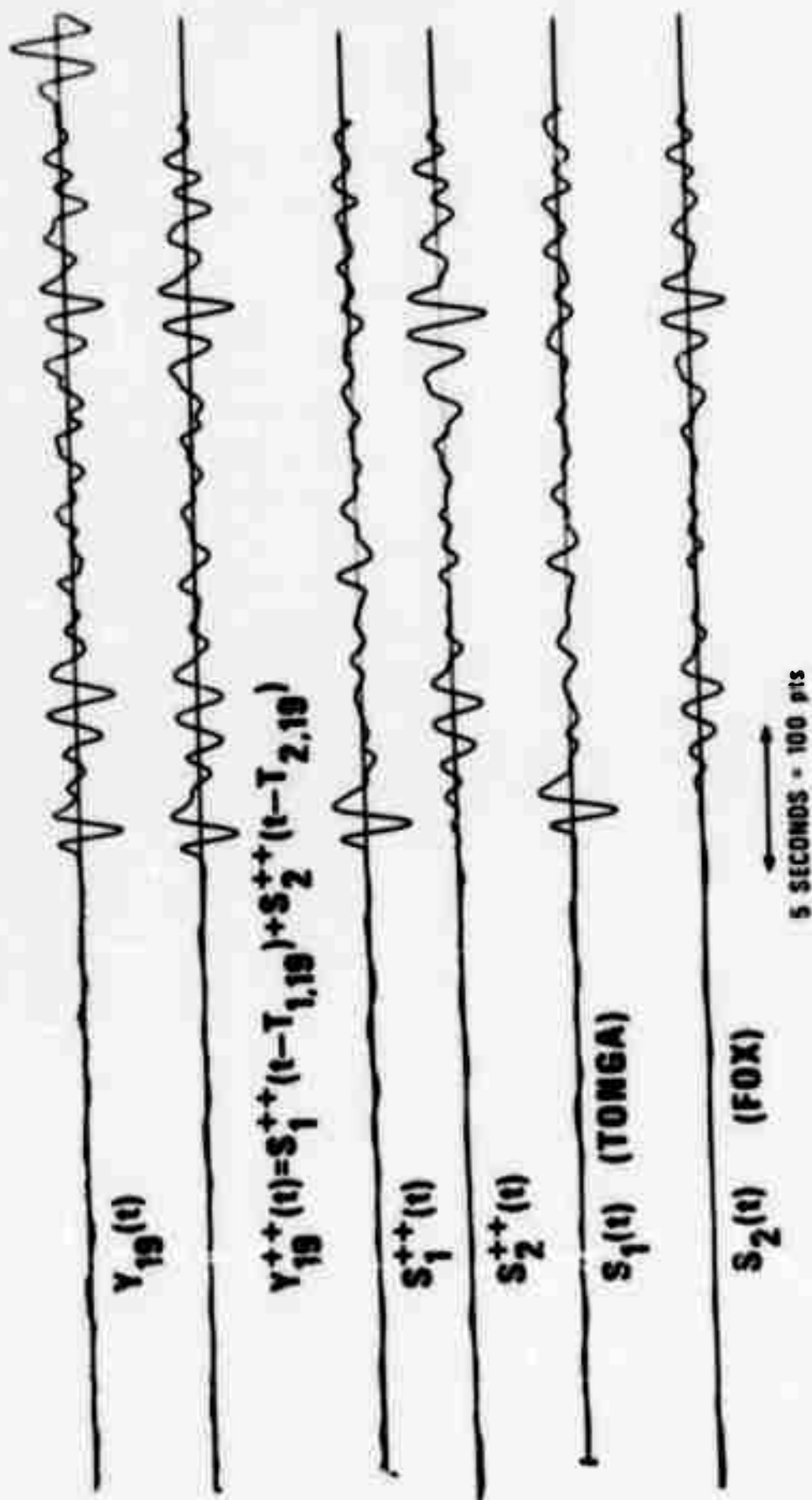


Figure 8. Analysis of Tonga,  $S_1(t)$  - Fox  $S_2(t)$  mixture using  $N = 19$  channels recorded at TFO at a high signal to noise ratio. Channels are normalized to equal peak-to-peak amplitude.

TABLE II

Values of F Testing for the Presence of the Fox Island  
Signal in Data Containing Both Fox Island and Tonga Signals.

<u>Hz (cps)</u>	<u>F</u>
.156	.84619
.313	45.39547
.469	26.19131
.625	58.49830
.781	10.86142
.938	24.44770
1.094	14.68781
1.250	13.02673
1.406	5.83217
1.563	5.08383
1.719	2.93364
1.875	2.95517
2.031	1.54600

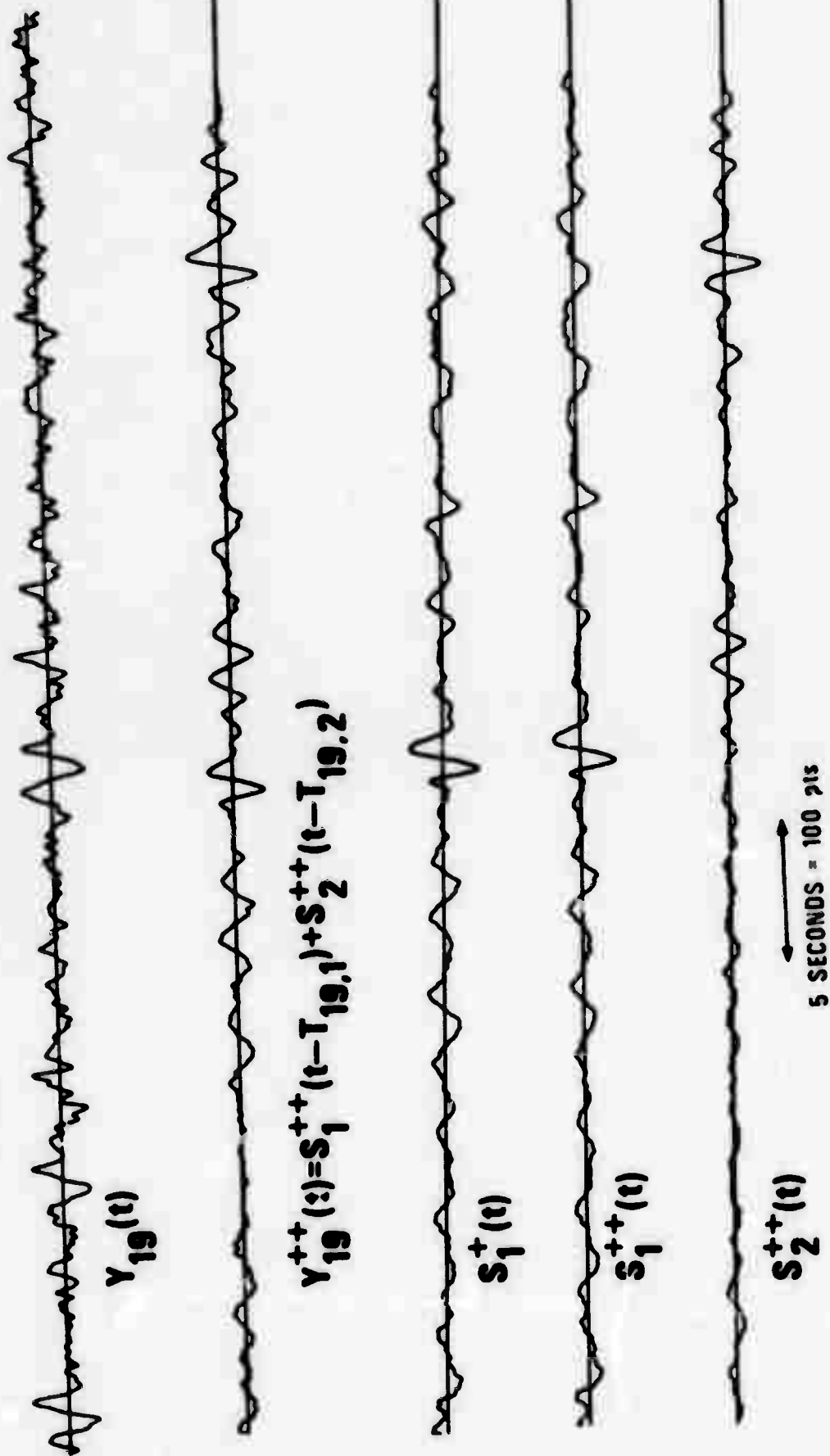


Figure 9. Analysis of Tonga  $S_1(t)$  and Fox  $S_2(t)$  noisy mixture using  $N = 19$  channels recorded at TFO. Channels are normalized to equal peak-to-peak amplitude.

TABLE III

Values of F Testing for the Presence of the Fox Island Signal  
in Noisy Data Containing Both Fox Island and Tonga Signals

<u>Hz (cps)</u>	<u>F</u>
.156	6.82573
.313	2.74730
.469	2.82802
.625	14.48280
.781	6.45614
.938	8.83391
1.094	5.37031
1.250	3.99074
1.406	1.34506
1.563	1.24787
1.719	1.51457
1.875	.40499
2.031	.91461

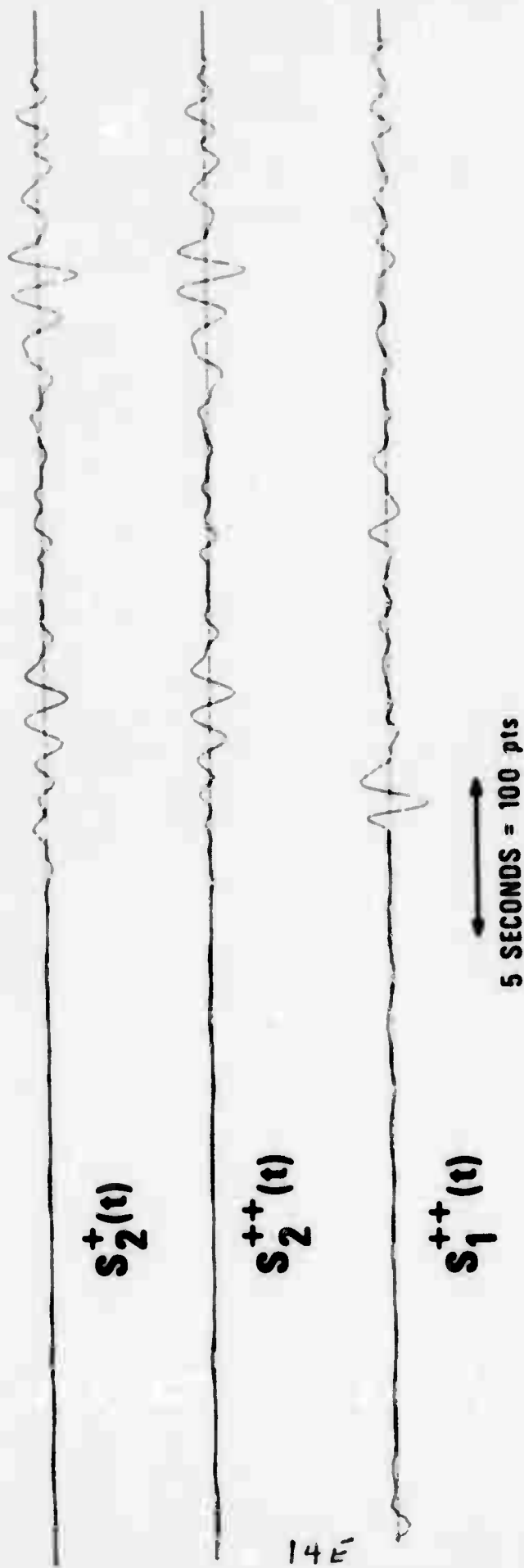
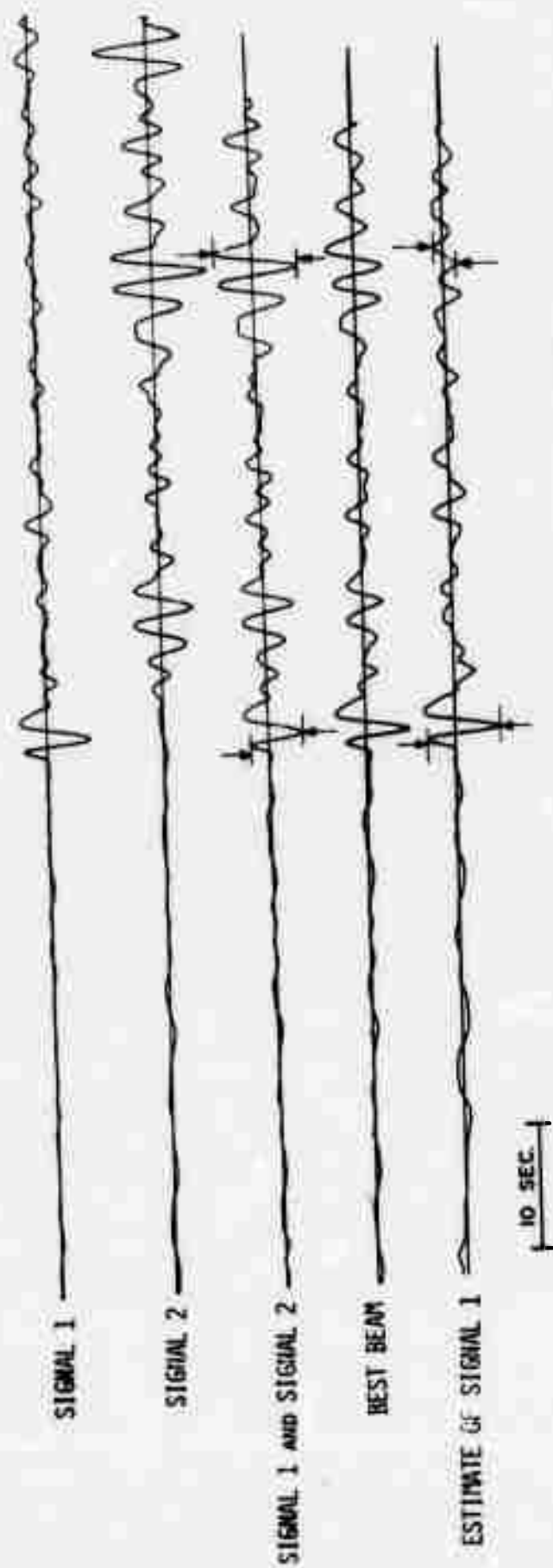


Figure 10a. Analysis of Tonga  $S_1(t)$  and Fox  $S_2(t)$  mixture for  $N = 19$  channels showing bias in beam formed estimate for Fox. Channels are normalized to equal peak-to-peak amplitude.

shows up in the value of the F statistic at 1.25 Hz. An even greater improvement over signal beamforming can be seen in Figure 10b in which the data are from the seven center elements at TFO.

In order to examine further the detection and estimation capability of the two-signal model for a somewhat smaller array, we again chose the seven center elements at TFO and investigated the process of testing for Tonga in the presence of Fox. A number of possible azimuths were tried for Tonga assuming that Fox was fixed at 17 km/sec and 308 degrees. This enables one to examine the sensitivity of the F statistic in resolving the azimuth of the Tonga signal in much the same way as a frequency wave number spectrum. Figures 11 and 12 show the high resolution frequency wave number spectra for the seven center elements, for the ordinary and noisy cases corresponding to the data in Figures 8 and 9 respectively. Figure 11 shows that Tonga and Fox may be resolved fairly well by conventional methods into two separate components. Figure 12 shows that the ability to distinguish two signals is diminished considerably by noisy data. Therefore, we might consider searching a reasonable collection of azimuths to look at the estimation and resolution capabilities of the maximum likelihood procedure. Figure 13 shows the estimates for the waveform of Tonga which would be obtained for various possible assumed azimuths if the seven center elements at TFO were used on data with a high signal to noise ratio. By comparing the waveform obtained with the true version in Figure 8, we note that



# SEVEN CHANNEL SHORT PERIOD TWO-SIGNAL MODEL

Figure 10b. Results of a least-squares technique for estimation of one signal in the presence of another. Channels are normalized to equal peak-to-peak amplitude.

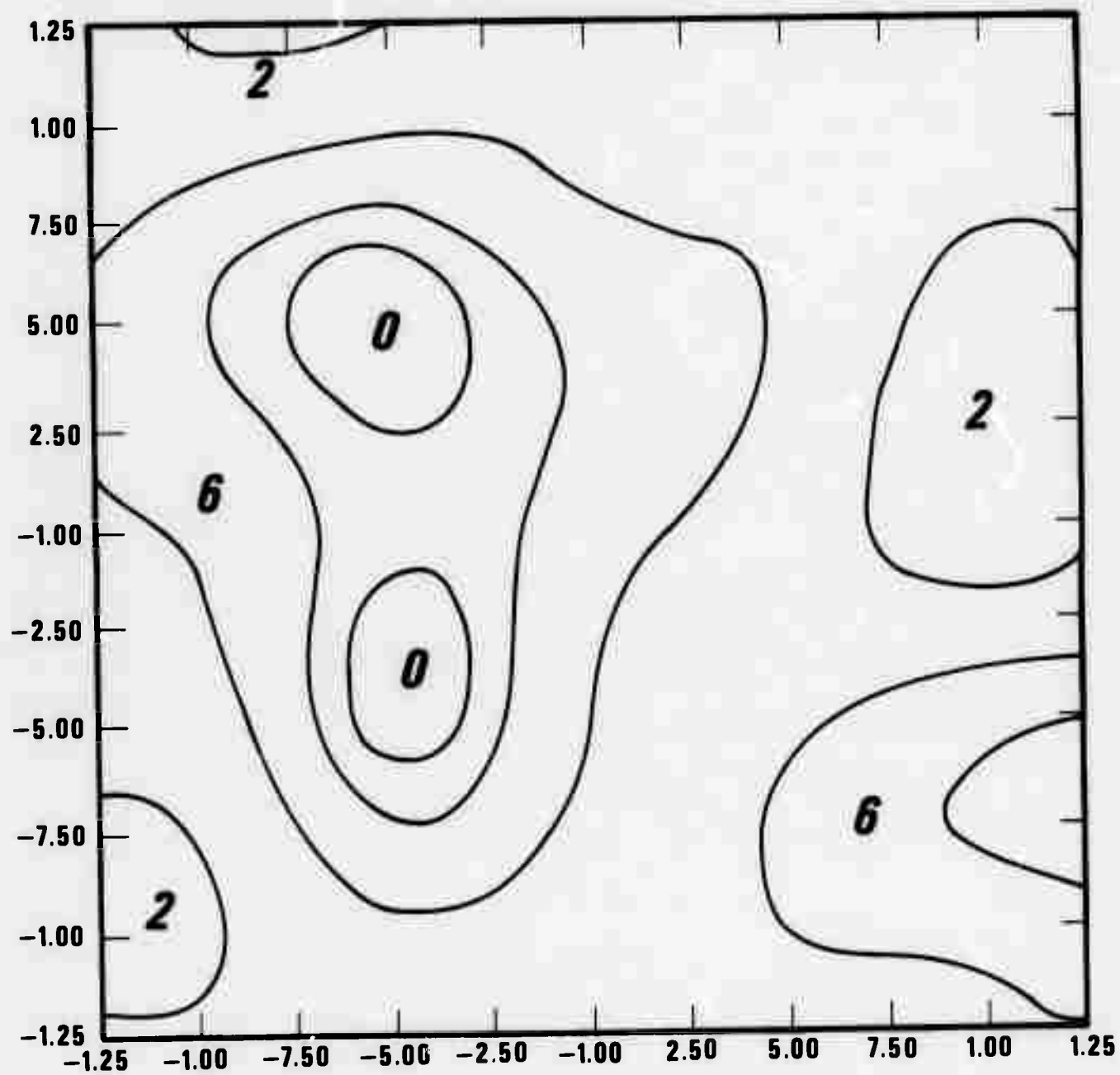


Figure 11. Frequency wave number analysis  $N = 7$  channels measuring Tonga and Fox at TFO (1.25 Hz).



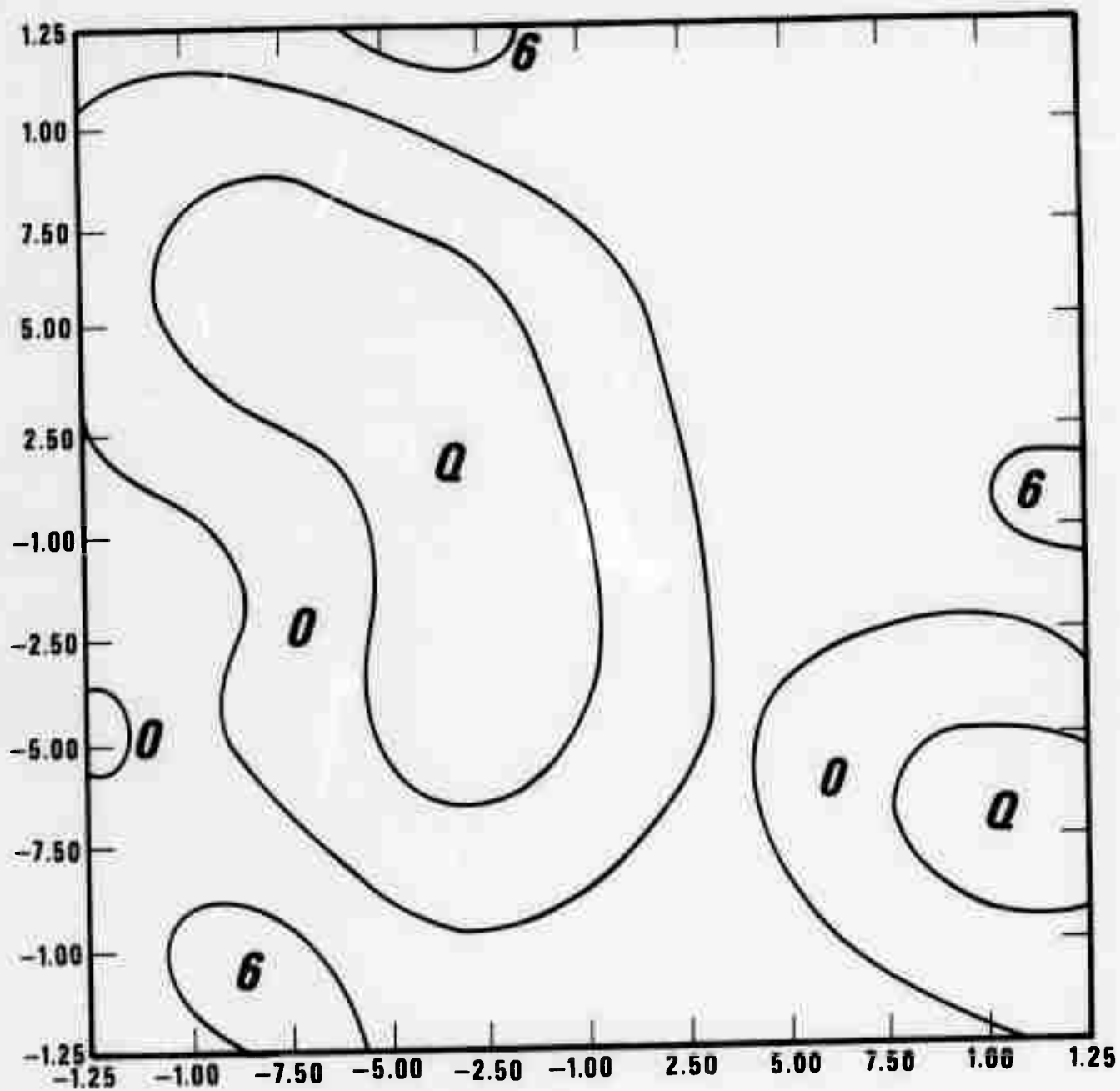


Figure 12. Frequency wave number analysis  $N = 7$  noisy channels measuring Tonga and Fox at TFO (1.25 Hz).

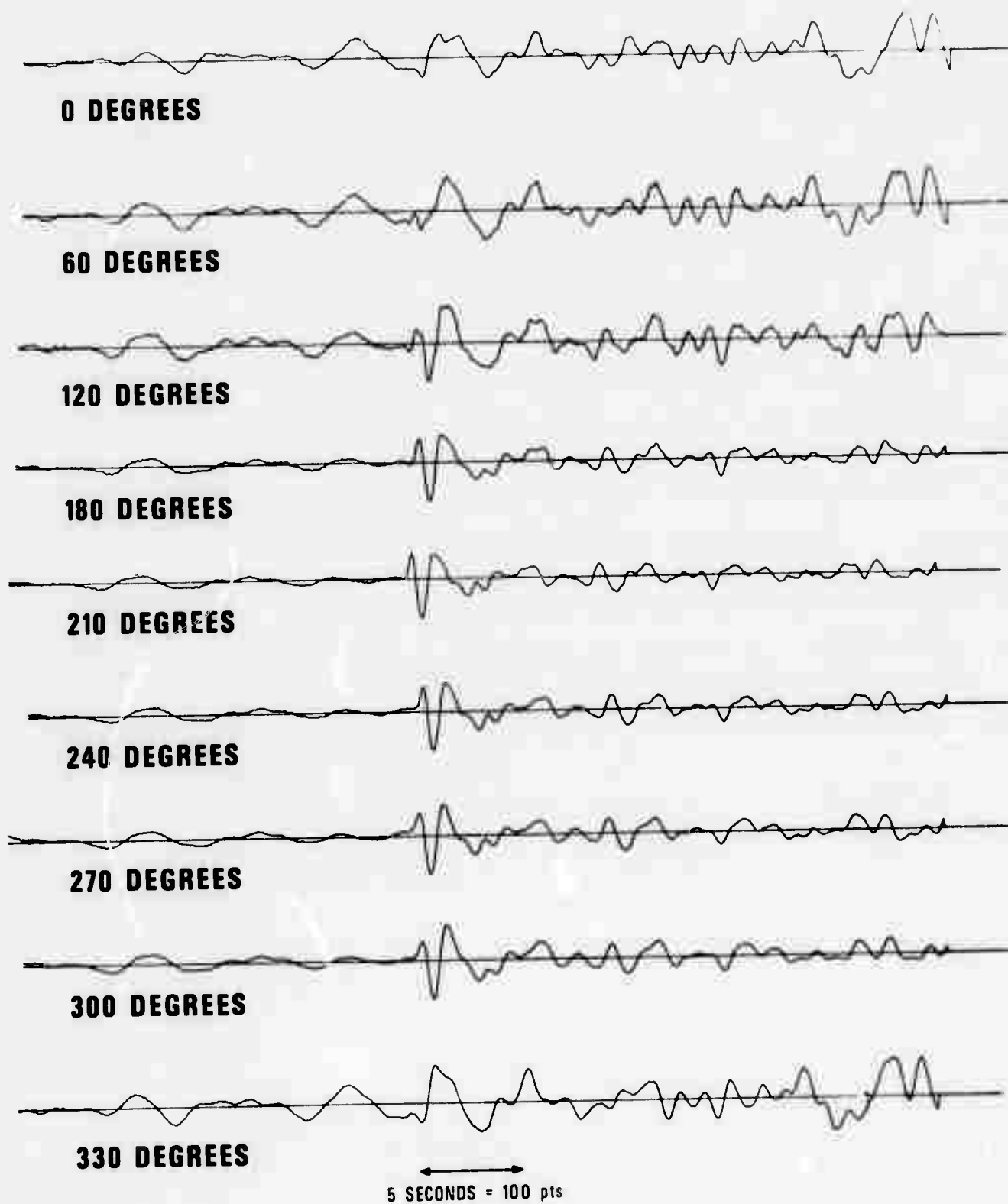


Figure 13. Maximum likelihood estimate for Tonga using Tonga-Fox mixture in  $N = 7$  channels at TFO (Figure 8) with various possible azimuths for Tonga. Channels are normalized to equal peak-to-peak amplitude.

reasonable estimates are obtained using any azimuth in the range 180-300 degrees. Definitive information on the detector is available in the plot of the F statistic against azimuth shown in Figure 14. In this case, values of F at the frequencies 1.25 Hz and 1.41 Hz exceed the .001 significance level (i.e. we would expect only 1 false alarm per 1000 frequencies or per 1000 reported experiments at one frequency) for azimuths between 180 and 280 degrees with the peak occurring between 230 and 240 degrees. This agrees with the approximate azimuth read from the F-K plot (Figure 11). The two procedures appear to work equally well in this case as the width of the main peak is about 10 degrees in either case.

No comparisons will be made on the relative dropoff in db for these procedures since the important measures in detection are not the absolute units in which a test statistic is expressed, but rather the probability that the test statistic would exceed the specified threshold when the signal is not there. For example, the comparison of the capability of a detector which uses peak to peak amplitude with a detector which computes the ratio of the signal power to the noise power cannot be made on the basis of the values for these two test statistics, but must be made on the basis of their probability distributions under presence or absence of the signal.

A noisy case (Figure 9) produces for the seven channel case the estimates for the Tonga waveform shown in Figure 15. In this case, the only evidence of the Tonga signal is a slight downward deflection at the

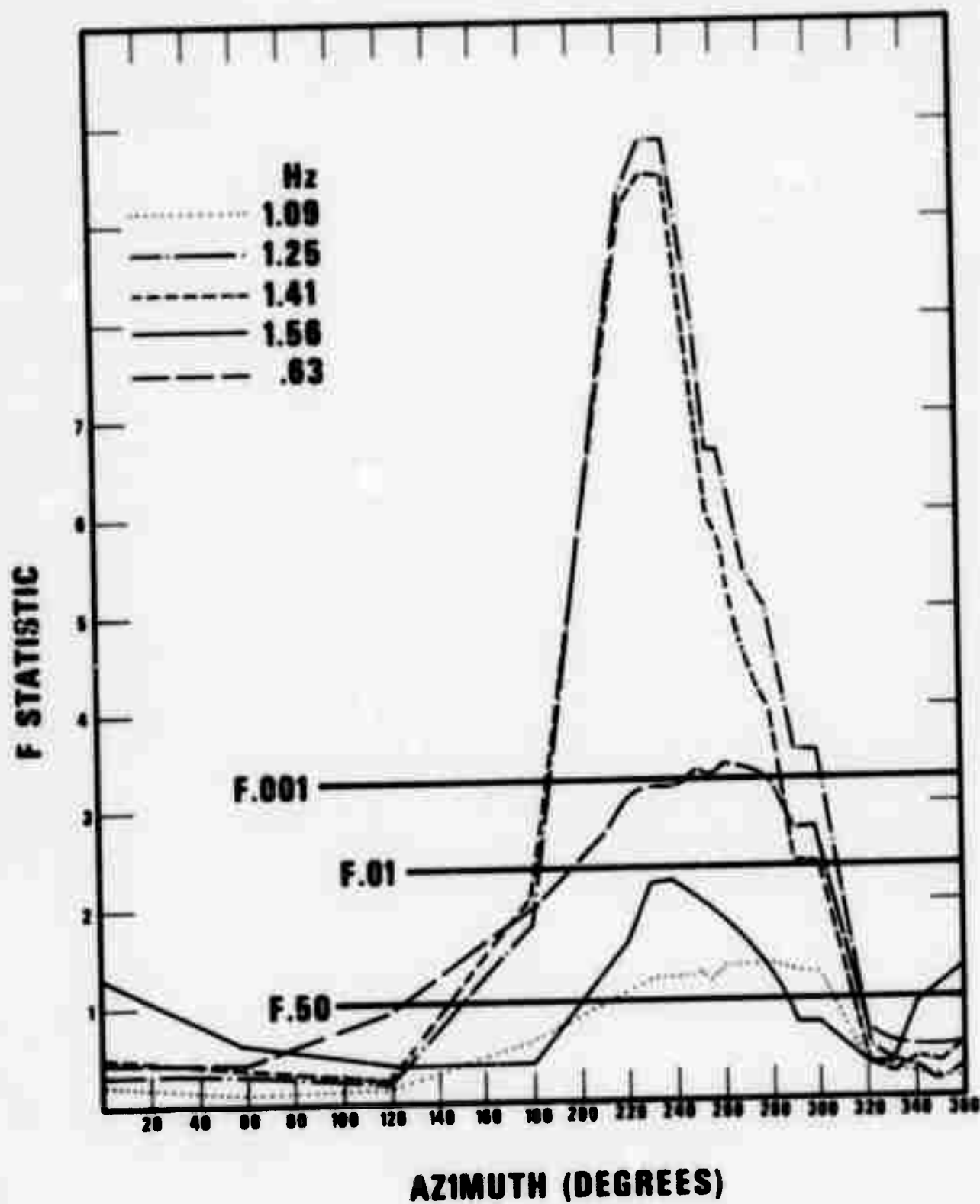


Figure 14. F statistics for detecting Tonga in Tonga-Fox mixture ( $N = 7$  center elements at TFO).



**180 DEGREES**



**240 DEGREES**



**300 DEGREES**



5 SECONDS = 100 pts

Figure 15. Maximum likelihood estimate for Tonga using Tonga-Fox mixture in  $N = 7$  noisy channels at TFO with various possible azimuths for Tonga. Channels are normalized to equal peak-to-peak amplitude.

point where Tonga should appear. The plot of the F statistic, Figure 16 however, clearly exhibits a peak (significant at .001 level) at 220 degrees azimuth. In fact, the F statistic exceeds the .01 threshold between 190 and 270 degrees as in the high signal to noise ratio case.

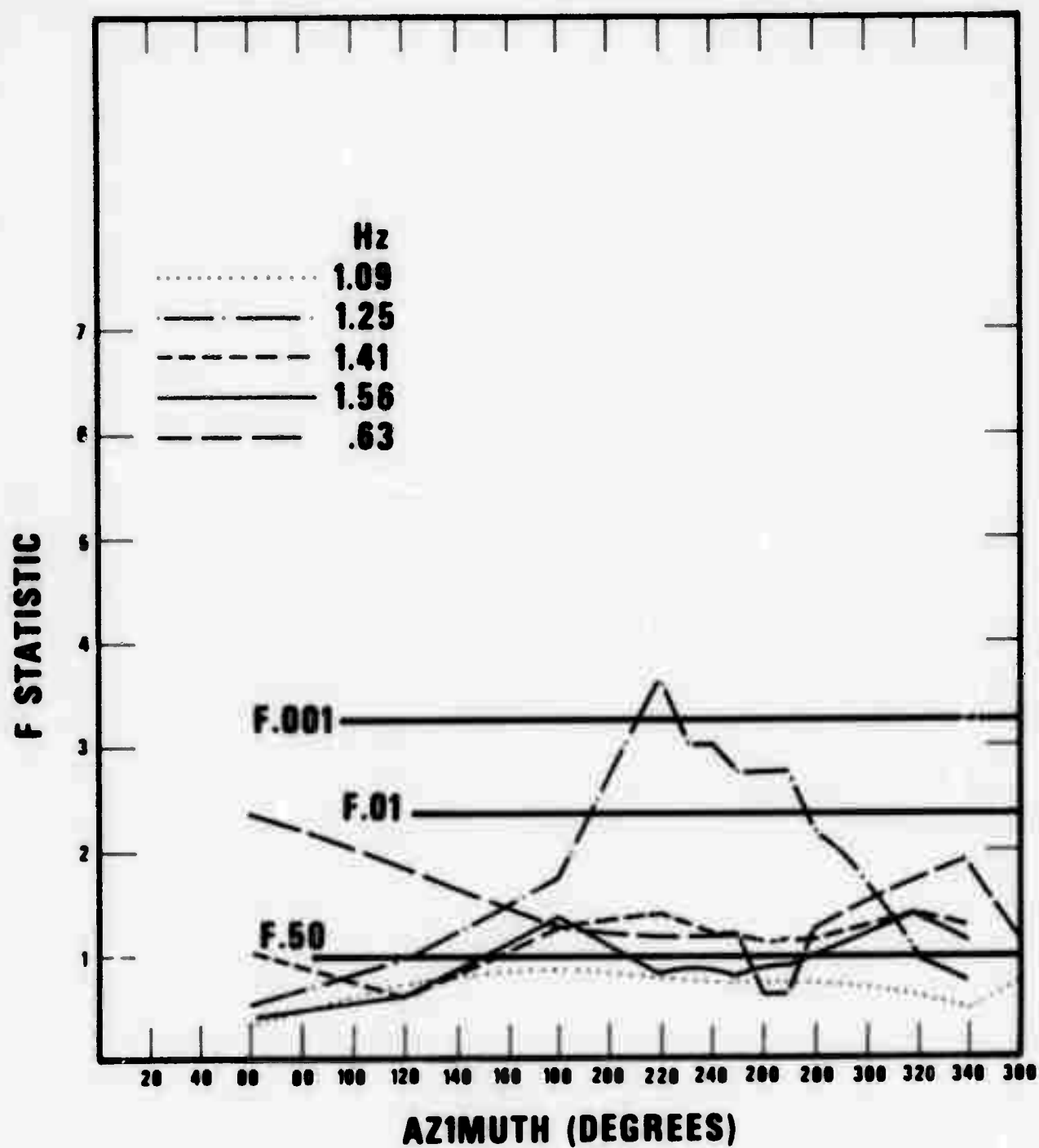


Figure 16. F statistic for detecting Tonga in Tonga-Fox noisy mixture (N = 7 center elements at TF0).

## SUMMARY

An investigation has been made of the effectiveness of truncated likelihood filters in simultaneously estimating and detecting two real seismic signals mixed with noise. It is found that the maximum likelihood filters give better estimates than simple beam forming, with the superiority most pronounced in small arrays. A theoretical procedure for examining the distortion of maximum likelihood and beamformed filters is derived and illustrated. The detection capabilities of the F statistic are examined for a small seven element short period array at TFO. A comparison with high resolution FK spectra shows that the two-signal version of the F statistic may be superior in the case where the noise level is high.



## REFERENCES

- Bendat, J.S. and Piersol, A., 1966, Measurement and analysis of random data: Wiley.
- Booker, A.H., 1965, Analysis of variance as a method for seismic signal detection: Seismic Data Laboratory Report NO. 116, Teledyne Geotech, Alexandria, Virginia.
- Blandford, R.R., 1970, An automatic event detector at TFO: Seismic Data Laboratory Report No. 263, Teledyne Geotech, Alexandria, Virginia.
- Capon, J., Jr., Greenfield, R. and Kolker, ., 1967, Multidimensional maximum likelihood processing of a large aperture seismic array: Proceedings of the IEEE, v. 55, p. 192-211.
- Dean, W.C., 1966, Rayleigh wave rejection by optimum filtering of vertical arrays: Seismic Data Laboratory Report No. 166, Teledyne Geotech, Alexandria, Virginia.
- Goodman, N.R., 1963, Statistical analysis based on a certain complex multivariate normal distribution: Ann. Math. Stat., v. 36, p. 152-172.
- Kelly, E.J., 1965, Signal parameter estimation for seismeter arrays: Lincoln Lab.
- Kobayashi, H. and Welch, P.D., 1970, The detection and estimation of two simultaneous seismic events: Proceedings of the Symposium on Computer Processing in Communication, Polytechnic Press, Brooklyn, New York.

## REFERENCES (Cont'd.)

- Hannan, E.J., 1971, Multiple time series: Wiley.
- Hannan, E.J., 1962, Regression for time series: In M. Rosenblatt ed. Time Series Analysis, Wiley.
- Melton, Ben S. and Bailey, Leslie F., 1957, Multiple signal correlators: Geophysics, v. 22, No. 3, p. 565-588.
- Schweppe, R., 1968, Sensor array data processing for multiple signal sources: IEEE Transactions on Information Theory, v. IT-14, p. 294-305.
- Shumway, R.H. and Dean, W.C., 1968, Best linear unbiased estimation for multivariate stationary processes: Technometrics, v. 16, p. 523-534.
- Shumway, R.H. and Husted, H.L., 1970, Frequency dependent estimation and detection for seismic arrays: Seismic Data Laboratory Report No. 242, Teledyne Geotech, Alexandria, Virginia.
- Shumway, R.H., 1970, Applied regression and analysis of variance for stationary time series: J. Am. Stat. Assoc., v. 65, No. 332, p. 1927-1946.
- Shumway, R.H., 1971, On detecting a signal in N stationarily correlated noise series: Technometrics, (in press).